Supplementary Information to

Understanding therapeutic tolerance through a mathematical model of drug-induced resistance

Jana L. Gevertz, James M. Greene, Samantha Prosperi, Natacha Comandante-Lou, and Eduardo D. Sontag

S.1 Rate Approximation

We have fit the two-compartment model (1)- (2) to obtain parameter values as a function of dose; see Table 1 for the estimated parameters $\theta = \theta(u)$, where

$$\theta(u) := (r_S(u), d_S(u), \alpha(u), r_R(u), d_R(u)). \tag{S1}$$

Recall that the drug-induced delay terms ($\gamma_{1,2}$) were not fit, but fixed at a value of 0.01 per hour. Our work in Sections 2.1 and 2.3 suggests that linearly interpolating the rate parameters θ with respect to the logarithm (base 10) of the dose provides close agreement to the experimental data. Thus, utilizing such an interpolation, we can obtain expressions for the rate parameters for *all* doses between $0.032\ \mu$M and $3.2\ \mu$M:

$$\theta(u),\ u \in [0.032, 3.2]\ \mu\text{M}. \tag{S2}$$

This interpolation is shown in Figure 6.

In order to solve an optimal control problem, it is numerically advantageous to assume that the vector field is smooth. More specifically, we will utilize CasADI [1], an open-source framework for nonlinear optimization and optimal control, which relies on the Interior Point Optimizer (Ipopt) software package to solve nonlinear programming problems. Here multiple shooting methods are utilized to transform the original optimal control problem to a constrained nonlinear programming problem, which is then solved via Ipopt. As Ipopt implements an interior line search method, it assumes that the objective is at least twice continuously differentiable [2], which is generally not satisfied by the function $\theta(u)$ in Figure 6; recall $\theta(u)$ is derived from piecewise-linear interpolation on the logarithm of the doses. Thus, we approximate the piecewise-linear rate functions by degree three polynomials using standard least-squares regression; the original and approximating expressions are provided in Figure S1. As the polynomial approximations closely match the piecewise-linear curves (in both the logarithmic and linear scales), for the optimal control portions of this manuscript, we define $\theta(u)$ by the polynomial approximations in Figure S1.

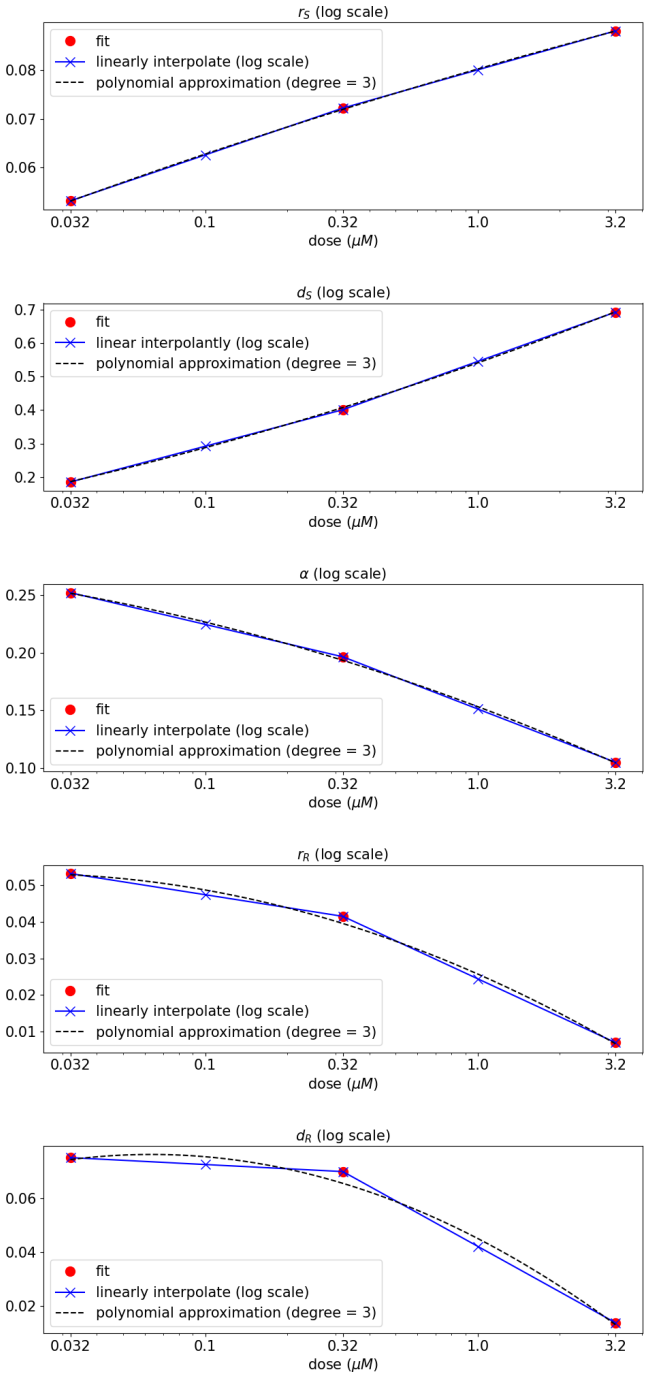

Supplementary Figure S1: Rate parameters r_S, d_S, α, r_R, and d_R in system (1) - (2) as a function of dose u. Red circles denote fits from experimental data, blue crosses denotes piecewise-linear interpolation (on the log scale with respect to dose), and the dotted black curve denotes a third-degree polynomial approximation to the data. Compare to Figure 6.

S.2 Near-Optimal Parameters for Two- and Three-Population Models

2-Pop	**0.032 µM**		**0.32 µM**		**3.2 µM**	
Model	Optimal	Near-Optimal*	Optimal	Near-Optimal*	Optimal	Near-Optimal *
r_S	0.0722	0.0693 - 0.0772	0.0722	0.0693 - 0.0772	0.0880	0.0831 - 0.0889
d_S	0.1855	0.1690 - 0.2188	0.4012	0.3712 - 0.4516	0.6924	0.6462 - 0.7000
α	0.2520	0.2467 - 0.3579	0.1963	0.1737 - 0.2518	0.1048	0.0773 - 0.1204
r_R	0.0532	0.0498 - 0.0546	0.0415	0.0353 - 0.0445	0.0070	0.0001 - 0.0219
d_R	0.0751	0.0691 - 0.0779	0.0699	0.0581 - 0.0752	0.0137	0.0001 - 0.0417

Supplementary Table S1: Best-fit and near-optimal parameters ranges using the two-population model in equations (1)-(2). *Of the 1000 best-fit parameters identified from the multi-start fitting algorithm, the number identified as near optimal is: 201 for the dose of 0.032 μM, 422 for the dose of 0.32 μM, and 507 for the dose of 3.2 μM.

3-Pop	**0.032 µM**		**0.32 µM**		**3.2 µM**	
Model	Optimal	Near-Optimal*	Optimal	Near-Optimal*	Optimal	Near-Optimal *
r_S	0.0530	0.0507 - 0.0550	0.0716	0.0675 - 0.0769	0.0881	0.0837 -0.0890
d_S	0.1650	0.0714 - 0.1896	0.3709	0.3229 - 0.4355	0.6926	0.6466 - 0.7000
q	0.2691	0.2681 - 0.5990	0.2330	0.1981 - 0.3489	0.1067	0.0911 - 0.1266
β	0.0531	0.1026 - 0.5999	0.1689	0.0331 - 0.5992	0.3205	0.0001 - 0.6000
r_R	0.0530	0.0505 - 0.0537	0.0414	0.0356 - 0.0506	0.0069	0.0003 - 0.0890
d_R	0.0748	0.0701 - 0.0762	0.0696	0.0588 - 0.0856	0.0134	0.0043 - 0.6799

Supplementary Table S2: Best-fit and near-optimal parameters ranges using the three-population model in equations (4)-(6). *Of the 1000 best-fit parameters identified from the multi-start fitting algorithm, the number identified as near optimal is: 207 for the dose of 0.032 μM, 362 for the dose of 0.32 μM, and 655 for the dose of 3.2 μM.

S.3 Inclusion of Pre-Existing Resistance in Two-Population Model

Parameter	0.032 μM		0.32 μM		3.2 μM	
	$R(0) = 0$	$R(0) = 0.01$	$R(0) = 0$	$R(0) = 0.01$	$R(0) = 0$	$R(0) = 0.01$
r_S	0.0532	0.0532	0.0722	0.0725	0.0880	0.0886
d_S	0.1855	0.1869	0.4012	0.4044	0.6924	0.6967
α	0.2520	0.2514	0.1963	0.1963	0.1048	0.1040
r_R	0.0532	0.0532	0.0415	0.0413	0.0070	0.0068
d_R	0.0751	0.0752	0.0699	0.0696	0.0137	0.0133
ζ_{opt}	44.762	44.763	33.406	33.392	22.159	22.094

Supplementary Table S3: Comparison of best-fit parameters and optimal value of the cost function when there is no pre-existing resistance ($R_0 = 0$) compared to when 1% of cells are initially resistant to the drug ($R_0 = 0.01$).

S.4 A Variation on the Three-Population Model

Here, we introduce a three-population model in which quiescence is a terminal state, rather than a transitory state en route to resistance. To this end, we modified the original three-population model by allowing the drug to induce a fraction $0 \leq \pi \leq 1$ of sensitive cells (S) into a quiescent state (Q) and the remaining $1 - \pi$ into a resistant state R. Setting $\beta = 0$ in the original three-population model results in a model where both quiescence and resistance are possible terminal states. The equations are as follows:

$$\dot{S} = r_S S - d_S(1 - e^{-\gamma_1 t})S - \alpha(1 - e^{-\gamma_2 t})S \tag{S3}$$

$$\dot{Q} = \pi\alpha(1 - e^{-\gamma_2 t})S \tag{S4}$$

$$\dot{R} = (1 - \pi)\alpha(1 - e^{-\gamma_2 t})S + r_R R - d_R(1 - e^{-\gamma_1 t})R. \tag{S5}$$

The optimal fits of this model at a dose of 0.032, 0.32 and 3.2 μM are shown in Figure S2. The optimal parameterization is found in Table S4, *with parentheses showing optimal for the original three-population model*.

The optimal parameterization of this alternate three population model shows that, at low and intermediate doses, cells generally shuttle from S directly to R, skipping over Q (since π is small). Sensitive and resistant cell behavior is generally unchanged from the original model. At high dose, half of the cells go to Q while the other half go to R. The resistant cells behave quite differently than before - they grow very slowly, and are killed quite easily. As a result, the resistant population cannot be sustained (and S is naturally eliminated by drug), so the tumor is composed completely of quiescent cells by the end simulation time. This aligns with the results of the original three-population model, which predicted that resistant cells were categorized by such a low growth rate that they were effectively quiescent. Further, just like with the original three-population model, parameters lack identifiability in the alternate three-population model (Figure S3).

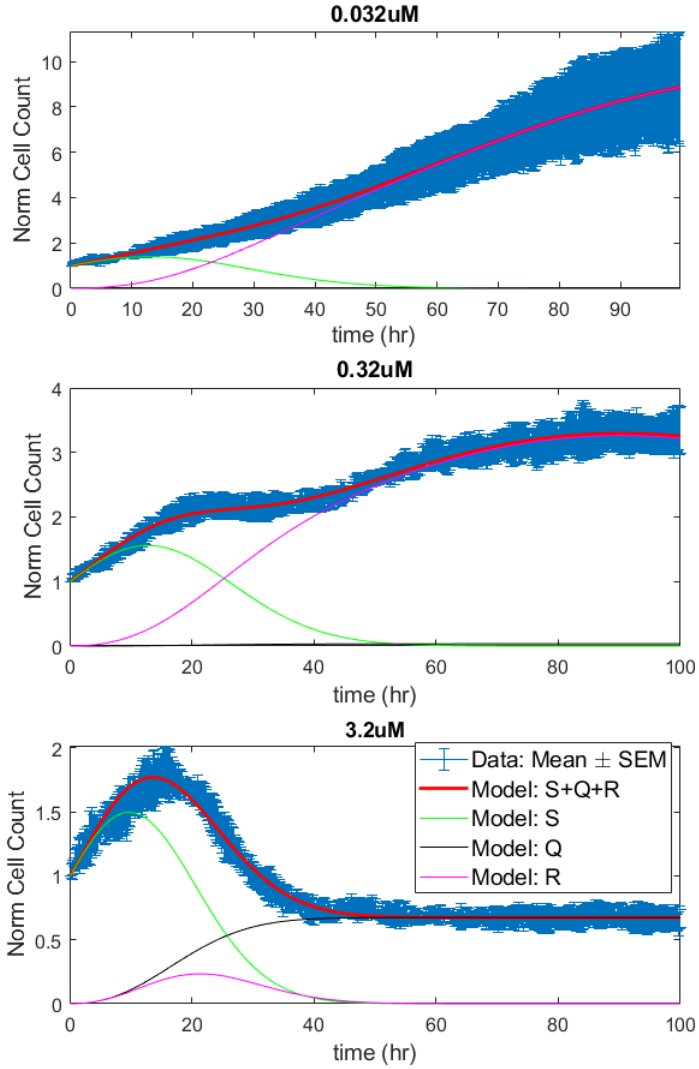

Supplementary Figure S2: Fits for revised three-population model.

Parameter	Drug Concentration		
	0.032 µM	**0.32 µM**	**3.2 µM**
r_S	0.0531 *(0.0530)*	0.0723 *(0.0716)*	0.0864 *(0.0881)*
d_S	0.1849 *(0.1650)*	0.4024 *(0.3709)*	0.6064 *(0.6926)*
α (compare to q)	0.2511 *(0.2691)*	0.1994 *(0.2330)*	0.3241 *(0.1067)*
π (no comparison)	1.477×10^{-4}	0.0239	0.4956
r_R	0.0531 *(0.0530)*	0.0418 *(0.0414)*	1.166×10^{-4} *(0.0069)*
d_R	0.0751 *(0.0748)*	0.0744 *(0.0696)*	0.6063 *(0.0134)*
ζ_{opt}	44.76 *(44.82)*	33.40 *(33.34)*	22.04 *(22.14)*

Supplementary Table S4: Best-fit parameters for revised three-population model. When applicable, the italic value in parenthesis specifies the best-fit value of the parameter in the original three-population model.

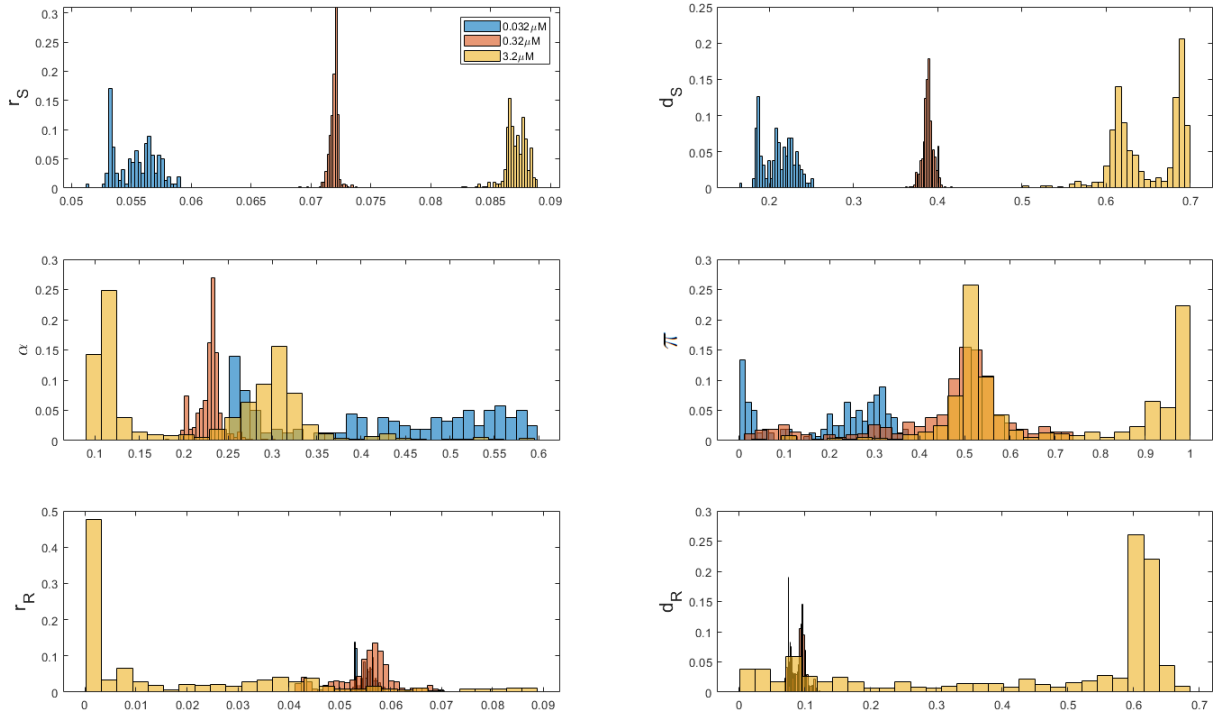

Supplementary Figure S3: Histograms for revised three-population model.

S.5 Comparisons With Other Mathematical Models

As discussed in Section 1, the mathematical model used in this paper is a modification of the one that we had introduced in [3] and further analyzed in [4]. Since the publication of [3], several alternative mathematical models of emergence of therapy resistance have been proposed by other authors, so it is useful to briefly review these and compare among them and to our original and revised models. We do that here.

The equations presented in the paper [5] model the dynamics of phenotypic adaptation in cell subpopulations, both on- and off-treatment, by a monoclonal antibody therapy (cetuximab, used on colorectal cancer cells). The equations during treatment are as follows:

$$\begin{aligned} \dot{S} &= \lambda S - \mu S - \delta_S e^{-kt} S \\ \dot{R} &= \lambda R + \mu S - \delta_R e^{-kt} e^{-wt} R \,. \end{aligned}$$

The cell proliferation rate λ is assumed to be the same in both sensitive (S) and resistant (R) populations. When the treatment is on, S cells may acquire resistance, and they switch to R cells at a rate μ. Cytotoxic effects on S and R are modeled by two linear terms, $-\delta_S e^{-kt}$ and $-\delta_R e^{-kt}$ respectively. The efficacy of the drug is assumed here to diminish at an exponential rate e^{-kt}, because of the declining function of effector cells such as NK cells. The term e^{-wt} is used to model transience of resistance, which evolves under selective pressure at rate w. When the treatment is off, a different set of equations is used. In this regime, resistant R cells switch back to sensitive cells S at a rate of $\tilde{\mu}$, but no cell death is assumed:

$$\begin{aligned} \dot{S} &= \lambda S + \tilde{\mu} R \\ \dot{R} &= \lambda R - \tilde{\mu} R \,. \end{aligned}$$

In contrast to our model, the rates of death of both the S and R subpopulations decrease with time (more for R than for S due to the term e^{-wt} representing transience of resistance), and the growth rates are the same for both subpopulations.

The paper [6] employs a simpler model of resistance to targeted therapy (particular, the EGFR inhibitor gefitinib) or classical chemotherapy (paclitaxel). The authors focus on the fact that, under therapy, tumor volume initially decreases, but eventually increases again due to resistance. There is one tumor volume (or total number of tumor cells) equation, which can also be found in [7]:

$$\dot{V} = \left(\lambda - \delta e^{-kt}\right) V \,.$$

Here, $\delta > 0$ quantifies the maximum drug effect, which occurs at the beginning of treatment. This effect exponentially decreases as resistance arises, and $\lambda > 0$ represents the net growth rate after the drugs have lost its effect due to resistance. It is assumed that $\delta > \lambda$, so that at small times, prior to the emergence of resistance, the drugs are effective (negative net growth rate). Observe that, in contrast to our model and the model in [5], there is a single tumor volume equation instead of separate equations for sensitive and resistant cells. Interestingly, if we set $\delta_R = \delta_S = \delta$ and $w = 0$ (no transience of resistance) in the model in [5] then we recover these models from [6, 7] for the total cell population $V = S + R$.

The paper [8] employs a tumor growth model to evaluate patient-specific resistance to radiation combined with pembrolizumab and bevacizumab treatments for high-grade glioma. There are two equations, one for tumor growth dynamics and one for the death rate:

$$\begin{aligned} \dot{V} &= (\lambda - \gamma) V \\ \dot{\gamma} &= -k\gamma \,. \end{aligned}$$

where k indicates the rate at which resistance develops. With $\delta = \gamma(0)$, this can be summarized by $dV/dt = (\lambda - \delta e^{-kt})V$, which is the same model as in [6, 7].

The paper [9] has a more complex model, involving three subpopulations: sensitive (S), persister (P), and resistant (R):

$$\begin{aligned} \dot{S} &= \lambda_S (1 - \beta C) S \log(K/V) \\ \dot{P} &= \lambda_P (1 - \mu) P \log(K/V) \\ \dot{R} &= \lambda_R R \log(K/V) + \lambda_P \mu P \log(K/V) \,. \end{aligned}$$

Here K is a carrying capacity term, $V = S + P + R$, λ_i are the Gompertz growth rate constants in the absence of drug, a proportionality term βC models death of sensitive tumor cells as a function of drug plasma concentration $C(t)$, and the persister population P transitions to the resistant compartment with a mutation probability μ. This model differs from ours in many ways, including the Gompertz growth term (we tested Gompertz models and obtained poorer fits to our data), the lack of delays for drug action, and the use of three compartments, which we found did not improve fits to COLO858 response to vemurafenib *in vitro*.

The paper [10] focuses on melanoma adaptive therapy through two ODE models of interactions between drug-sensitive and resistant cells. In a first model, drug-sensitive (S) and drug-resistant (R) subpopulations compete for limited resources through a classical Lotka-Volterra competition for resources mechanism:

$$\begin{aligned} \dot{S} &= \lambda_S \left(1 - \frac{S + R}{K}\right) S - \delta S \\ \dot{R} &= \lambda_R \left(1 - \frac{cS + R}{K}\right) R \,. \end{aligned}$$

Here K is a carrying capacity and the parameter c quantifies the degree to which sensitive cells inhibit the growth rate of resistant cells in comparison to resistance cells among themselves. The authors assume that $\lambda_S = 0$ during treatment, because they model BRAF/MEK inhibitors which are assumed to act through growth inhibition as well as apoptosis (δ term). An alternative model proposed in the same paper sets $c = 1$ but incorporates phenotypic switching between drug-sensitive and drug-resistant cells, with induced transitions from sensitive to resistant states (term αS) or vice-versa (term βR):

$$\begin{aligned} \dot{S} &= \lambda_S \left(1 - \frac{S + R}{K}\right) S - \alpha S + \beta R - \delta S \\ \dot{R} &= \lambda_R \left(1 - \frac{S + R}{K}\right) R + \alpha S - \beta R \,. \end{aligned}$$

It is assumed that the transition rate constant α is non-zero during treatment, and is zero otherwise, and that the transition rate constant β is nonzero when treatment is off and is zero otherwise. This model is similar in many ways to our model in [4], which is cited in [10], but with several important differences, including the fact that the population-switching terms are only active during therapy or not, and that R cells are fully resistant (no death term).

The paper [11] developed a model for induced resistance of colorectal cancer cells to targeted therapies. The model has sensitive (S) and drug-tolerant persister (P) populations:

$$\begin{aligned} \dot{S} &= \Big(\lambda_S - \delta_S(u(t)) - \lambda(u(t))\Big) S \\ \dot{P} &= -\delta_P P + \lambda(u(t)) S \,. \end{aligned}$$

Drug-treated cells can die, replicate, or switch to a persister state P at a rate λ in a dose-dependent fashion $\lambda(u(t))$. $u(t)$ is the amount of drug at time t, and it is either constant or linearly increasing (see [11], Supplementary Information, Extended Data Figure 5). Resistant cells are not explicitly modeled, because it is assumed that persisters that attempt to divide before acquiring drug-resistance mutations die, and thus a possible back-switching from persister to sensitive populations in the presence of drug would simply be incorporated into their death rate. Note that the death rate $\delta_S(u(t))$ of sensitive cells is assumed to be drug-dependent, but that of persister cells is not. This model differs from ours in many ways, including the fact that we have delays in drug action and phenotype transitions, and that a reverse phenotype transition back to sensitive type is non-negligible (and needed for fits). Note, however, that our three-population equations with a "quiescent" population could be thought of as having a persister compartment.

In summary, although different, these models share important features with ours, although they differ in important ways. For additional discussion, see also the review article [12].

S.6 Optimal Control as a Function of Total Applied Dosage

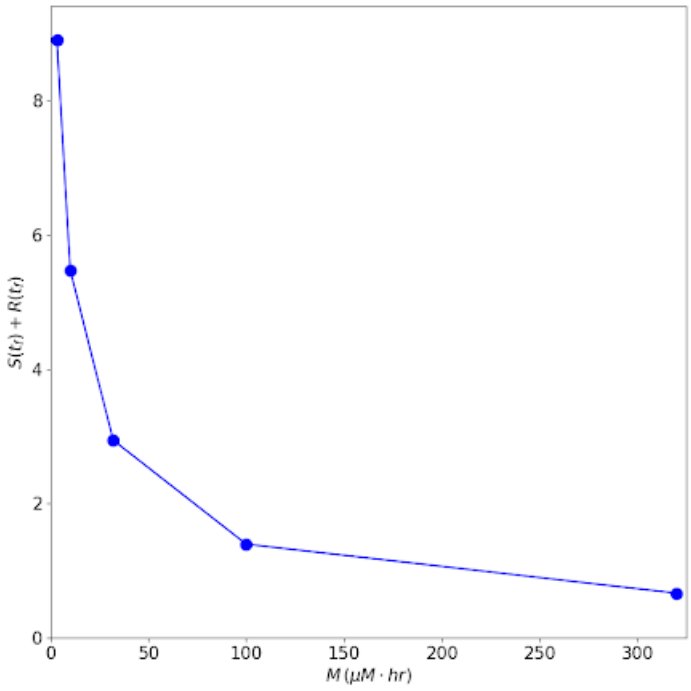

Supplementary Figure S4: Optimal tumor size, as determined by the optimal control problem posed in Section 4.5, as a function of total dosage.

References

[1] J. A. E. Andersson, J. Gillis, G. Horn, J. B. Rawlings, and M. Diehl, "CasADi – A software framework for nonlinear optimization and optimal control," *Mathematical Programming Computation*, vol. 11, no. 1, pp. 1–36, 2019.

[2] A. Wächter and L. T. Biegler, "Line search filter methods for nonlinear programming: Motivation and global convergence," *SIAM Journal on Optimization*, vol. 16, no. 1, pp. 1–31, 2005.

[3] J. Greene, C. Sanchez-Tapia, and E. Sontag, "Mathematical details on a cancer resistance model," *Frontiers in Bioengineering and Biotechnology*, vol. 8, pp. 501: 1–27, 2020.

[4] J. Greene, J. Gevertz, and E. Sontag, "Mathematical approach to differentiate spontaneous and induced evolution to drug resistance during cancer treatment," *JCO Clin. Cancer Inform.*, vol. 3, pp. 1–20, 2019.

[5] J. Zhou, C. Liu, Y. Tang, Z. Li, and Y. Cao, "Phenotypic switching as a non-genetic mechanism of resistance predicts antibody therapy regimens," *iScience*, vol. 27, Apr 2024.

[6] M. Nagase, S. Aksenov, H. Yan, J. Dunyak, and N. Al-Huniti, "Modeling tumor growth and treatment resistance dynamics characterizes different response to Gefitinib or chemotherapy in non-small cell lung cancer," *CPT Pharmacometrics Syst Pharmacol*, vol. 9, pp. 143–152, Mar 2020.

[7] L. Claret, P. Girard, P. M. Hoff, E. Van Cutsem, K. P. Zuideveld, K. Jorga, J. Fagerberg, and R. Bruno, "Model-based prediction of phase iii overall survival in colorectal cancer on the basis of phase ii tumor dynamics," *Journal of Clinical Oncology*, vol. 27, no. 25, pp. 4103–4108, 2009. PMID: 19636014.

[8] D. J. Glazar, G. D. Grass, J. A. Arrington, P. A. Forsyth, N. Raghunand, H.-H. M. Yu, S. Sahebjam, and H. Enderling, "Tumor volume dynamics as an early biomarker for patient-specific evolution of resistance and progression in recurrent high-grade glioma," *Journal of Clinical Medicine*, vol. 9, no. 7, 2020.

[9] C. Grassberger, I. McClatchy, David, C. Geng, S. C. Kamran, F. Fintelmann, Y. E. Maruvka, Z. Piotrowska, H. Willers, L. V. Sequist, A. N. Hata, and H. Paganetti, "Patient-Specific Tumor Growth Trajectories Determine Persistent and Resistant Cancer Cell Populations during Treatment with Targeted Therapies," *Cancer Research*, vol. 79, pp. 3776–3788, 07 2019.

[10] E. Kim, J. S. Brown, Z. Eroglu, and A. R. Anderson, "Adaptive therapy for metastatic melanoma: Predictions from patient calibrated mathematical models," *Cancers*, vol. 13, no. 4, 2021.

[11] M. Russo, S. Pompei, A. Sogari, M. Corigliano, G. Crisafulli, A. Puliafito, S. Lamba, J. Erriquez, A. Bertotti, M. Gherardi, F. Di Nicolantonio, A. Bardelli, and M. Cosentino Lagomarsino, "A modified fluctuation-test framework characterizes the population dynamics and mutation rate of colorectal cancer persister cells," *Nature Genetics*, vol. 54, pp. 976–984, Jul 2022.

[12] J. W. T. Yates and H. Mistry, "Clone wars: Quantitatively understanding cancer drug resistance," *JCO Clinical Cancer Informatics*, vol. 4, pp. 938–946, 2020. PMID: 33112660.